RSC Advances

This study was to clarify the pathogenesis of CRF and action mechanism of TAES.

1   **A Urine Metabonomics Study of Chronic Renal Failure and Intervention Effects**

2   **of Total Aglycone Extracts of *Scutellaria Baicalensis* in 5/6 Nephrectomy Rats**

3

4   Junwei Fang [a,1], Wenyu Wang [a,b,1], Shujun Sun [a], Yang Wang [a], Qianhua Li [a], Xiong

5   Lu [c], Zhihui Hao [d], Yongyu Zhang [a,]*

6   [a] *Center for Traditional Chinese Medicine and Systems Biology, Shanghai University*

7   *of Traditional Chinese Medicine, Shanghai 201203, China*

8   [b] *MacroStat (China) Clinical Research Co., Ltd, Shanghai 201203, China*

9   [c] *Experiment Center for Science and Technology, Shanghai University of Traditional*

10   *Chinese Medicine, Shanghai 201203, China*

11   [d] *Laboratories of Biological Pharmaceutical, College of Chemical and*

12   *pharmaceutical Sciences, Qingdao Agricultural University, Qingdao, 266109, China*

13   **Abstract**

14   Chronic renal failure (CRF) is a severe disease that can lead to decline of life quality. *Radix*

15   *Scutellariae* is a well-known traditional Chinese medicine (TCM). Our previous study has

16   demonstrated that the Total Aglycone Extracts of *Scutellaria Baicalensis* (TAES), can improve

17   renal fibrosis induced by mercuric chloride in rats. However, no research has investigated the

18   efficacy and mechanism of TAES in treating CRF. In the present study, we investigated the effects

19   of TAES on some closely related parameters in 5/6 nephrectomy CRF rats, and studied the

20   pathogenesis of CRF and the mechanism of TAES treatment using a metabonomics method based

21   on gas chromatography coupled with mass spectrometry (GC/MS). Rats with CRF were divided

22   into six groups with rats subjected to sham operation as normal control. After eight weeks of

23   treatment by TAES, the levels of serum creatinine (Scr) and blood urea nitrogen (BUN) were

Abbreviation: TAES, Total Aglycone Extracts of *Scutellaria Baicalensis*

* Corresponding Authors at: Center for Traditional Chinese Medicine and Systems Biology,
Shanghai University of Traditional Chinese Medicine, 1200 Cailun Road, Shanghai 201203, China.
Tel.: 86 21 51322748.

E-mail address: dryyz@sina.com (Yongyu Zhang)

[1] These authors contributed equally to this work

24　　decreased, and the metabolic perturbations induced by 5/6 nephrectomy were reversed according

25　　to pattern recognition analysis. Meanwhile, 18 potential biomarkers associated with CRF were

26　　identified, and the affected metabolic pathways in 5/6 nephrectomy rats were extracted based on

27　　the differential metabolites. Our findings suggest that TAES have positive effects on 5/6

28　　nephrectomy-induced CRF in rats and show therapeutic potentials in CRF treatment. Our findings

29　　also indicate that metabonomics analysis based on GC/MS is a useful tool for studying the effect

30　　of drugs on the whole body, exploring biomarkers involved in CRF and elucidating the potential

31　　therapeutic mechanisms of TCM.

32

33　　**Keywords:** Metabonomics, GC/MS, Total aglycone extracts of *scutellaria baicalensis*, Chronic

34　　renal failure, 5/6 nephrectomy

35　　**1 Introduction**

36　　Chronic renal failure (CRF) refers to the progressive renal injury resulted from primary or

37　　secondary chronic kidney diseases (CKD). It is often accompanied by a series of clinical

38　　syndromes and metabolic disorders, and could eventually develop into end stage renal disease

39　　(ESRD). Besides the increase in chronic diseases commonly observed in an expanding elderly

40　　population, such as hypertension, diabetes and abuse of nephrotoxic drugs, the prevalence and

41　　incidence of common disorders like CKD has also risen in past years, all of which impose a rising

42　　demand on the healthcare systems [1]. Currently, there is no effective treatment for CRF due to its

43　　unclear pathogenesis [2]. Therefore, it is of great significance to study CRF pathogenesis and to

44　　develop effective drugs for the treatment of CRF. The rat model 5/6 nephrectomy is characterized

45　　by glomerulosclerosis, tubular injury and interstitial fibrosis. Due to its similar pathological

46　　process with human CRF, 5/6 nephrectomy is commonly used to study CRF pathogenesis [3] and

47　　potential mechanisms of drug effect [2].

48　　Metabonomics is a branch of system biology that is based on the analysis of an entire spectrum of

49　　metabolites rather than focusing on individual ones. Unbiased measurement and holistic analysis

50　　of biological samples are the critical steps of metabonomics studies. Due to its powerful separation

51　　efficiency and detection sensitivity, gas chromatography coupled with mass spectrometry (GC/MS)

52 is considered as one of the most useful approaches in the field of metabonomics research [4,5].

53 For example, metabonomics studies using GC/MS have been widely adopted in the evaluation of

54 therapeutic efficacy of traditional Chinese medicine (TCM) [6].

55 *Radix Scutellariae* is a well-known TCM with the efficacy for heat-clearing, dampness-drying,

56 fire-purging, detoxicating, maintaining hemostasis and preventing abortion [6]. It is listed in the

57 Pharmacopoeia of the People's Republic of China and mainly contains flavonoids such as baicalin,

58 wogonoside, baicalein, wogonin and oroxylin A [7,8,9]. *Radix Scutellariae* also has a higher

59 content of glycosides (also known as baicalin, wogonoside, et al.) than that of aglycones (also

60 known as baicalein, wogonin, et al.). Several studies showed that the glycosides in *Radix*

61 *Scutellariae* could be absorbed only after it has been hydrolysed to flavonoid aglycones by

62 intestinal flora [10,11]. We have previously hydrolysed flavonoid glycoside to aglycones using

63 enzymes found within *Radix Scutellariae*, and then extracted total flavonoid aglycone with ethyl

64 acetate. We optimized the methodology of the extraction process and obtained the corresponding

65 Chinese patent (CN 1583775A).

66 The key to treating CRF is to protect the function of residual kidney tissues. Many clinical and

67 experimental studies declared that TCM processes unique protecting effects on renal function in

68 patients with CRF [12]. It has been reported that Total Aglycone Extracts of *Scutellaria*

69 *Baicalensis* (TAES) can improve renal fibrosis induced by mercuric chloride in rats [13]. However,

70 the potential efficacy and mechanism of TAES as a treatment for CRF induced by 5/6

71 nephrectomy remain unclear. In order to fill this knowledge gap, we studied the pharmacology of

72 TAES intervention in 5/6 nephrectomy rats, analyzed the pathogenesis of CRF in a holistic

73 environment using metabonomics and explored the efficacy and mechanism of TAES on CRF.

74   **2 Experimental**

75   2.1 Chemicals

76   Losartan Potassium Tablets were purchased from MSD of Hangzhou in China. Methoxyamine

77   hydrochloride, N,O-Bis (trimethylsilyl) trifluoroacetamide (BSTFA + TMCS 99 : 1), urease and

78   Myristic acid were purchased from Sigma Corporation of America. Chloral hydrate, heptanes,

79   methanol, anhydrous ethanol, ethyl chloroformate, pyridine, and chloroform were of analytical

80   grade and were supplied by China National Pharmaceutical Group Corporation in Shanghai, China.

81   L-2-Chlorophenylalanine and heptadecanoic acid, used as internal quality standards, were

82   provided by Sigma Corporation of America. The ultrapure water was obtained from Milli-Q

83   system (Millipore, USA).

84   2.2 Preparation of TAES

85   Dried Scutellaria was purchased from Inner Mongolia. The effective fraction (EF) used in the

86   present study was extracted by ethyl acetate after a three-hour enzymolysis at 37°C using enzyme

87   present in Scutellaria. The total content of baicalein, wogonin and oroxylin-A in the EF was more

88   than 60%. The extraction process of the EF is protected by the Chinese patent (CN 1583775A).

89   2.3 Animals and 5/6 nephrectomy

90   105 male Wistar rats weighing 180 ± 10 g were purchased from Shanghai Sippr BK Laboratory

91   Animals Ltd. (Shanghai, China). All rats were housed in an air-conditioned room at 20 - 25°C with

92   a 12 h light / 12 h dark cycle. The animals were allowed free access to food pellets and water. All

93   experimental procedures were approved by the Ethics Committee of the Institute of Shanghai

94   University of TCM. After one week, 5/6 nephrectomy was performed as described previously [14].

95   Briefly, rats were put under anesthesia with chloral hydrate (300 mg/kg body weight, i.p.). Then

96   approximately 2/3 of the left kidney was ablated and then the right renal pedicle was ligated seven

97   days later.

98   2.4 Groups and Treatment

99   Animals were randomly divided into 7 groups, namely, one control group, one positive group, one

100   model group and four treatment groups, with 15 animals in each group. The rats that underwent a

4

101   sham operation were used as normal control (sham group). Rats in the four treatment groups were

102   orally administered 10, 20, 40 and 80 mg/kg•d TAES by intubation, respectively. The positive

103   group received losartan (20 mg/kg•d). The same volume of distilled water was given to the sham

104   and control groups. All rats were sacrificed after eight weeks of successive treatments. Overnight

105   (24 h) urine samples of 8 randomly selected rats from each group were collected in metabolic

106   cages at week 0 (pre-dose), and at 2, 4, 6 and 8 weeks after 5/6 nephrectomy. All urine samples

107   were stored at −80°C. The animals were anesthetized with chloral hydrate and blood was obtained

108   from the abdominal aorta for renal function analysis. The kidneys were isolated and fixed with 10%

109   buffered formalin for histological study.

110   2.5 Assays for Serum creatinine (Scr) and Blood urea nitrogen (BUN)

111   Levels of Scr and BUN were measured using an Automatic Biochemical Analyzer (HITACHI

112   7080, JAP).

113   2.6 Histological Study

114   A portion of the kidney tissue was trimmed, fixed with 10% buffered formalin, and embedded in

115   paraffin for light microscopy analysis. Sections with a thickness of 3 μm were stained with

116   haematoxylin and eosin stain.

117   2.7 Urine sample preparation and GC/MS assay

118   All the urine samples were thawed in ice water bath and vortex-mixed before analysis. Each 600

119   μL aliquot of standard mixture or urine sample was added to a screw tube. After adding 100 μL of

120   l-2-chlorophenylalanine (0.1 mgmL^{-1}), 400 μL of anhydrous ethanol, and 100 μL of pyridine to

121   the urine sample, 50 μL of ECF were added for first derivatization at 20.0 ± 0.1℃. The pooled

122   mixtures were sonicated at 40 kHz for 60 s. Then, extraction was performed using 300 μL of

123   chloroform, with the aqueous layer pH was carefully adjusted to 9-10 using 100 μL of NaOH (7

124   mol L^{-1}). The derivatization procedure was repeated with the addition of 50 μL ECF into the

125   aforementioned products. After the two successive derivatization steps, the overall mixtures were

126   vortexed for 30 s and centrifuged for 3 min at 3000 rpm. The aqueous layer was aspirated off, and

127   the remaining chloroform layer containing derivatives was isolated and dried with anhydrous

5

128 sodium sulfate and subsequently subjected to GC-MS analysis.

129 Sample analysis by GC/MS was performed according to our previously published work with

130 minor modification [15]. All GC-MS analyses were performed by a mass spectrometer 5975B

131 (Agilent technologies, USA) coupled with an Agilent 6890 (Agilent technologies, USA) gas

132 chromatography instrument. In the gas chromatographic system, a capillary column (Agilent J&W

133 DB-5ms Ultra Inert 30 m × 0.25 mm, film thickness 0.25 μm) was used. Helium carrier gas was

134 injected at a constant flow rate of 1.0 mL × min^{-1}. Derivatized samples of 1 μL each were injected

135 into the GC/MS instrument in splitless injection mode. A programmed column temperature was

136 optimized for successful separation (Table 1). The temperatures of the injection port, interface, and

137 the source were set at 260°C, 280°C and 230°C, respectively. The measurements were collected

138 using electron impact ionization (70 eV) in full scan mode (m/z 30 – 550). The solvent post time

139 was set to 5 min.

140 **Table 1** Temperature program of column incubator in GC/MS.

Rate (℃/min)	Temperature (℃)	Hold time (min)
	70	2
5	120	0
3	190	0
5	210	0
10	260	0
5	290	0

141 2.8 Data analysis

142 All results were presented as mean ± SD. Data were analyzed using SPSS 13.0 statistical package.

143 Data for multiple comparisons were performed by one-way ANOVA followed by Dunnett's test. A

144 value of $P < 0.05$ was considered statistically significant.

145 All the GC/MS raw files were converted to NetCDF format using Data Bridge software

146 (Perkin-Elmer Inc., USA), and were subsequently processed using XCMS toolbox

147 (http://metlin.scripps.edu/download/) with default settings for baseline correction, peak

148 discrimination and alignment. The resulting data were exported into Microsoft Excel, and the

149   peaks were normalized to the total sum of spectrum prior to multivariate analyses. The data were

150   analyzed by principal component analysis (PCA), partial least squares-discriminate analysis

151   (PLS-DA) and orthogonal partial least squares (OPLS) using SIMCA-P 11.5 software (Umetrics,

152   Umea, Sweden) after undertaking a unit variance procedure. The concentrations of potential

153   biomarkers were represented as relative areas using the internal standard areas as reference. For

154   GC/MS data, significant variables (markers) are selected based on a threshold of a multivariate

155   statistical parameter, such as variable importance in the projection (VIP) value from an OPLS

156   model. The higher the VIP values, the greater influence the variables have on the discrimination

157   between the two groups. Variables with VIP values exceeding 1 are first selected. In a second step,

158   those differential metabolites are validated at a univariate level with Mann-Whitney U test. The

159   threshold of p value is usually set to 0.05. These variables, then, were identified by searching in

160   NIST database and verified by standards.

161   **3. Results**

162   3.1 Effects of TAES on BUN and Scr levels. Fig. 1 shows the effects of TAES on parameters

163   indicative of renal function. Compared with the sham group, the levels of BUN (A) and Scr (B)

164   were dramatically increased in the control group after eight weeks of water treatment. However,

165   the BUN and Scr levels were decreased after eight weeks treatment with TAES (10, 20, 40 and 80

166   mg/kg•d) in comparison with those of the control group.

167   3.2 Histological Findings. Histological examination further confirmed renal dysfunction in 5/6

168   nephrectomy animals (Fig. 2). B shows features of renal tissues from the model group compared

169   with those from the sham group (A). These features include disordered glomerular structure,

170   hyperemia, interstitial cell hyperplasia, severe inflammatory cell infiltration, and fibrous tissue

171   hyperplasia. In contrast, these changes were significantly reversed after eight consecutive weeks

172   of TAES treatment.

173   3.3 Metabonomics analysis

174   Urine data of sham group and model group before operation were analyzed by PCA and PLS-DA. .

175   Automatic modeling parameters indicated the poor explanation and predication of the models as

7

176   shown in Table 2, meaning that there was no difference in urine metabolism between these two

177   groups (Table 2). The time-related metabolic pattern of PLS-DA scores is shown in Fig. 3. In both

178   the model and the sham groups, distinct metabolic changes were apparent from week 0 onwards,

179   suggesting that age might have an influence on urine metabolism in rats. For more reliable

180   comparison, urine metabolism analysis should base on samples collected at the same time across

181   different treatment groups.

182   **Table 2** Automatic modeling parameters for the classification of sham operation group versus model group before
183   model establishment.

Model	Amount of components	R^2X	R^2Y	Q^2Y
PCA-X	3	0.674		0.352
PLS-DA	0			

184   R^2X_{cum} and R^2Y_{cum} represent the cumulative sum of squares (SS) of all the X's and Y's explained by all extracted
185   components.
186   Q^2Y_{cum} is an estimate of how well the model predicts the Y's.

187   3.3.1 Analysis of metabolic profiles and identification of potential biomarkers.
188   Urine data of sham group and model group at the 8th week after operation, with the greatest

189   metabolism changes, were chosen to OPLS analysis. Based on the metabolic profiles, 18

190   metabolites, which related to the group separation with the parameter VIP (Variable Importance in

191   the Projection[16]) > 1, were selected as potential biomarkers (p < 0.05 Student's t-test) (Table 3).

192   Each of these potential biomarkers was further identified using the available reference compounds

193   and the commercial compound libraries NIST.

194   **Table 3** Potential biomarkers related to CRF.

Metabolites	Model/Sham	TAES40/Model
L-Cysteine	↑	↓△
Malate	↓	↓
Uracil	↓	↓
L-Alanine	↓	↓
L-Methionine	↑	↑
Cadaverine	↓	↓

L-Aspartate	↑	↑
Retinotic acid	↑	↓△
Creatinine	↑	↓△
Phenylacetic acid	↑	↓△
D-Ribose	↑	↓△
D-Mannitol	↑	↓△
Ribitol	↑	↑
D-galactonic acid	↓	↓
Myo-Inositol	↑	↑
D-Galactose	↑	↑
Xylitol	↑	↓△
D-Glucose	↑	↓△

195   The up and down arrows represent the relative increasing or decreasing trend of the metabolites in the model group

196   compared to those in the sham group or in the TAES40 group compared to the model group.

197   △ represents reverse trend compared to that in model /sham group.

198   3.3.2 Influence of lostartan on the urinary metabolic profiles

199   Sham operation group, model group and losartan group were distinguished by PLS-DA analysis

200   (Fig. 4). Sham group can be separated completely from the model group in 3D-PLS-DA score plot

201   with the losartan group between them (Fig. 4A). This result indicated that losartan might improve

202   kidney function to a certain degree . Samples plotted in one dimension are showed in Fig. 4B. It is

203   evident that the principle component (PC) 3 accounted mainly for the treatment efficacy of

204   losartan on CRF (Fig. 4B (c)). In the score plot of PC 1, CRF rats (including those in the model

205   group and loasrtan treatment group) were distinctly separated from those in the sham operation

206   group (Fig. 4B (a)), which might be implicative of disease formation. PC 2 suggested possible

207   undesirable effects of losartan on CFR rats (Fig. 4 B (b)), as the urine metabolic profile of losartan

208   treated group was different from that of the non-administrated groups (including both the model

209   and the sham group).

210   3.3.3 Influence of TAES on urinary metabolic profiles

211   PLS-DA analyses of sham, model and treatment groups were shown in Fig. 5. In the score plot of

212   PC 1, TAES treatment groups were separated from the sham and the model groups (Fig. 5A).

213   Nevertheless, the sham and the model groups were clearly separated from each other in the score

214   plot of PC 2. In addition, the treatment groups showed a trend of reversing to the sham group (Fig.

215   5 B). The results demonstrated that TAES might have other effects on rats in addition to providing

216   protection against CRF.

217   3.3.4 Time-dependent changes of metabolic profile

218   The time-related metabolic pattern of the score plot of PC 2 was shown in Fig. 6. In the TAES

219   treatment group, the metabolic pattern was indicative of recovery toward the baseline state from

220   week 2 onwards, suggesting that TAES might potentially reverse the 5/6 nephrectomy-induced

221   CRF changes in rats.

222   **4. Discussion**

223   The 5/6 nephrectomy rats are a well-characterized model for studying CRF. It shows features of

224   glomerulosclerosis and tubulointerstitial fibrosis, which result in kidney dysfunction and a

225   significant increase in Scr and BUN levels [2]. Glomerulosclerosis and tubulointerstitial fibrosis

226   are the common pathological changes typically observed at the final stage of progression to CRF.

227   In the current study, 5/6 nephrectomy rats showed significant increase in Scr, BUN and fibrous

228   tissue hyperplasia. RAAS inhibitors, such as angiotensin-converting enzyme inhibitors and ARBs,

229   are the first-line drugs for treatment of renal fibrosis [17]. In this study, the therapeutic effect of

230   TAES was compared with that of losartan, an ARB used as positive control. TAES showed similar

231   therapeutic effects as losartan, with regard to improving kidney dysfunction and inhibiting fibrosis

232   in 5/6 nephrectomy rats.

233   BUN and Scr are two main diagnostic markers for CRF. In the present study, the dramatical

234   increase of BUN and Scr in the model group indicated that the CRF animal model was

235   successfully established. However, the sensitivity of these markers may be relatively low in early

236   CRF diagnosis and accurate therapeutic effect evaluation. Hence, novel approaches for the

237   detection of CRF are urgently needed. The nontarget metabolomics provides a global view of the

10

238 organism and can be used to monitor metabolic alterations that occur in different pathological

239 processes. Metabolites biomarkers may have the potential to improve diagnostic, prognostication,

240 and therapy of interest.

241 Metabonomics is becoming widely popular among research studies that focus on evaluation of

242 drug efficacy and safety due to its ability to identify specific changes in the overall metabolic

243 spectrum. It is worth noting that, besides its therapeutic potential, losartan, as indicated by the

244 PLS-DA analyses of the sham, model and losartan treatment groups, might also have some

245 undesirable effects on CFR rats. Meanwhile, disease phenotypes of CRF, rather than the treatment

246 effect of losartan, are the main contributor to the classifications of sham, model and losartan

247 treatment groups. This indicates that CRF symptoms were not improved completely after 8

248 consecutive weeks of losartan treatment. However, the inference of the multi-effect of losartan on

249 CRF rats was based on the understanding of single-dimensional mapping of the overall metabolic

250 spectrum, and therefore, should be verified by future studies.

251 Metabonomics not only allows for the study of a static physical state at a particular time point, but

252 also reflects the body's dynamic response to medical intervention. In the current study, TAES

253 exhibited a time-effect relationship in the treatment of CRF, as the metabolic pattern of the TAES

254 40 treatment group followed a time-dependent recovery trend toward the baseline state.

255 Identifying the metabolic indices that change over time in response to a pharmacological

256 intervention and investigating their biological significance are extremely helpful in evaluating

257 drug-target effect.

258 Metabolite profiling focuses on the analysis of a group of metabolites that are related to a specific

259 metabolic pathway in certain biological states [18]. It has contributed greatly to understanding the

260 pathogenesis of diseases and their pharmacodynamics mechanism in a holistic way. The complex

261 nature of the pathogenesis of CRF has limited our understanding of the disease. As the

262 development of most kidney diseases often manifests as changes in metabolite composition [19],

263 metabonomics is a powerful tool for the study of CRF pathogenesis. Based on pattern recognition

264 analysis of metabolites, a clear separation of the model and the control group was achieved, and

11

265   18 differential metabolites related to group separation were found. In order to identify possible

266   pathways that are affected in CRF, metabolites contributing to the separation of the sham and the

267   model animals were analyzed using MetPA (Fig. 7). It is generally accepted that changes occurring

268   at the critical positions within a network would trigger a more severe impact on the pathway than

269   changes at marginal or relatively isolated positions [20]. In this study, the impact-value threshold

270   was set to 0.10. Any pathways that scored above this threshold were categorized as potential target

271   pathways. Metabolic pathway analysis using MetPA revealed that metabolites that are important

272   for the host response to CRF, are those responsible for galactose metabolism (Fig.7B (a)), cysteine

273   and methionine metabolism (Fig.7B (b)), retinol metabolism (Fig.7B (c)), alanine, aspartate and

274   glutamate metabolism (Fig.7B (d)) and inositol phosphate metabolism (Fig.7B (e)).

275   Drug target is usually identified as the key molecule involved in a particular metabolic or

276   signaling pathway that is specific to a disease [21]. In the current study, changes in metabolites

277   related to CRF in the TAES 40 group were analyzed. Compared with the model group, 8 different

278   metabolites in TAES 40 treatment group followed a reversing trend to the levels in the sham group

279   (Table 3). Based on MetPA analysis (Fig. 8), retinol, cysteine and methionine metabolisms are

280   potential targets for CRF drug design. Although, the key metabolites in these two pathways were

281   restored to levels observed in the sham group after TAES treatment, 10 other metabolites were not

282   affected by treatment with TAES. This may account for the failure in getting better curative effect

283   and will be followed up by further studies in our laboratory.

284   , Evaluating metabolites changes at a higher level, from pathway to network, allows for

285   understanding the biological significance of metabolites affecting the state of an organism.

286   Metabolites with a dramatic impact on the relevant pathways (Fig. 7 B) always play important

287   roles in the pathogenesis and possible complication of the disease. D-Galactose, a reducing sugar,

288   can be converted to aldose and hydroperoxide under the catalysis of galactose oxidase, resulting in

289   generation of a superoxide anion and oxygen-derived free radicals [22]. The excessive levels of

290   D-galactose have been reported to increase the free radical production in renal tissues [23], which

291   is associated with the oxidative renal injury and AGE/ALE renal accumulation in rats. Methionine

292   (Met) is an essential amino acid that is derived primarily from the diet. Homocysteine (Hcy)

12

293   (KEGG: C00155) is formed as a primary intermediate during the metabolism of Met, and it is the

294   critical intersection of two metabolizing pathways: remethylation and transsulfuration, which are

295   involved in the salvaging of Met and synthesis of cysteine (Cys), respectively (Fig.7 B(b)). The

296   increase of Cys and Met caused by CRF leads to abnormal increase of Hcy. Hcy is a toxic

297   non-protein forming sulfur-containing amino acid, which contributes to generation of ROS, RNS,

298   and reactive thiol species, thereby decreases the bioavailability of NO. These processes activate

299   the latent MMPs, and inactive the TIMP, leading to adverse cardiovascular remodeling [24]. It is

300   well-known that people with CKD have a remarkably elevated risk for cardiovascular disease

301   (CVD) [25,26], and hyperhomocysteinaemia was found to be highly prevalent and significantly

302   related to cardiovascular morbidity and mortality in patients with renal disease [27]. Under state of

303   renal disease, the reduction of transport function may result in a decreased content of Retinoic acid

304   (RA) in renal [28]. As such, we drew a hypothesis that the levels of RA in the renal of UUO rats

305   are low while the high levels of RA in urine may associate with the reduction of renal transport

306   function caused by disease. RA is an active metabolite of vitamin A, which is involved in various

307   physiological processes. Vitamin A deficiency can lead to increased expression of FN, LN and

308   collagen IV. Various studies reported that RA regulates the expression of ECM and plays a critical

309   role in fibrotic diseases [29,30]. A protective role of RA against renal fibrosis in UUO rats was

310   reported [31]. Alanine (Ala) is one of the major amino acids present in proteins, and catabolism of

311   Ala yields pyruvate and ammonia, thus, Ala provides a source of carbon for nitrogen

312   transamination [32]. It was shown that Ala promotes insulin secretion from the clonal β-cell line

313   BRIN-BD11 at a substantially greater rate than all other amino acids [33], and the reduction of Ala

314   may decrease transamination of the body and aggravate metabolism disorder of glucose and

315   energy. Inositol is a key metabolite of inositol phosphate metabolism (Fig. 7 B(e)).

316   Phosphoinositides have been investigated as an important agonist-dependent second messenger in

317   the regulation of diverse physiological events depending upon the phosphorylation status of their

318   inositol group [34]. Dysregulation of phosphoinositides formation as well as their metabolism are

319   associated with various pathophysiological disorders [35]. The relative intensity of inositol was

320   upregulated in the model group which may associate with glucose and lipid metabolic disorders

321   and exaggerated inflammatory response.

322 **5. Conclusion**

323 In this study, 5/6 nephrectomy-induced CRF rat model was used to investigate the effects of TAES

324 on CRF. According to pattern recognition analysis after eight weeks of TAES treatment, our

325 results indicate that TAES can improve renal function and reverse the metabolic perturbations

326 induced by 5/6 nephrectomy in CRF rats. Meanwhile, 18 potential biomarkers associated with

327 CRF were identified and the disturbed pathways in 5/6 nephrectomy rats were extracted based on

328 the differential metabolites. Our findings suggest that TAES have positive effects on 5/6

329 nephrectomy-induced CRF in rats and show therapeutic potentials in CRF treatment. Our findings

330 also indicate that metabonomics analysis based on GC/MS is a useful tool for studying the effect

331 of drugs on the whole body (including therapeutic and side effects), exploring biomarkers

332 involved in CRF and elucidating the potential therapeutic mechanisms of TCM.

RSC Advances Accepted Manuscript

14

339 **Reference**

[1] A.M. Torres, M. Mac Laughlin, A. Muller, A. Brandoni, N. Anzai, and H. Endou, Altered renal elimination of organic anions in rats with chronic renal failure, Biochimica et Biophysica Acta (BBA) - Molecular Basis of Disease. 1740 (2005) 29-37.

[2] J.R. Lu, H.Y. Han, J. Chen, C.X. Xiong, X.H. Wang, J. Hu, X.F. Chen, L. Ma, Protective Effects of Bu-Shen-Huo-Xue Formula against 5/6 Nephrectomy-Induced Chronic Renal Failure in Rats, Evidence-Based Complementary and Alternative Medicine. Doi:10.1155/2014/589846.

[3] Z.H. Sha, P. Fu, L. Zhou, W.X. Tang, F. Liu, J. Li, Experimental Research on chronic renal failure induced by 5/6 nephrectomy, Sichuan Journal of Zoology. 25 (2005) 632-634 (Chinese).

[4] X.J. Gou, Q. Tao, Q. Feng, J.H. Peng, S.J. Sun , H.J. Cao, N.N. Zheng, Y.Y. Zhang, Y.Y. Hu, P. Liu, Urinary metabonomics characterization of liver fibrosis induced by CCl_4 in rats and intervention effects of Xia Yu Xue Decoction, Journal of pharmaceutical and biomedical analysis. 74 (2013) 62-65.

[5] L.L. Song, H.Y. Liu, Y. Wang, et al. Application of GC/MS-based metabonomic profiling in studying the therapeutic effects of Huangbai–Zhimu herb-pair (HZ) extract on streptozotocin-induced type 2 diabetes in mice. Journal of Chromatography B, 997(2015) 96-104.

[6] H.L. Li, Research progress of scutellaria baicalensis, Chemical Engineering & Equipment. 4 (2008) 100-102 (Chinese).

[7] P. Parajuli, N. Joshee, A.M. Rimando, S. Mittal, A.K. Yadav. In vitro antitumor mechanisms of various Scutellaria extracts and constituent flavonoids, Planta medica. 75 (2009) 41-48.

[8] Y.Y. Zhang, Y. Guo, M. Onda, K. Hahimoto, Y. Ikeya, M. Okada and M. Maruno, Four flavonoids from Scutellaria baicalensis. Phytochemistry, 35 (1994) 511-524

[9] Y.Y. Zhang, Y. Guo, H. Ageta, Y. Harigaya, M. Onda, K. Hahimoto, Y. Ikeya, M. Okada, M. Maruno, Studies on the constituents of roots of Scutellaria planipes, Planta medica, 63 (1997) 536-539

[10] J. Xing, X.Y. Chen, D.F. Zhong, Absorption and enterohepatic circulation of baicalin in rats, Life Sciences. 78 (2005) 140-146.

[11] Q.M. Che, X.L. Huang, Y.M. Li, K. Zhang, H. Akao, X. Hattori, Studies on Metabolites of Baicalin in Human Urine, China Journal of Chinese Materia Medica. 26 (2001) 768-7699 (Chinese).

[12] L.M. Ai, X.P. Zhang, B.H. Li, Treatment status of chronic renal failure by traditional Chinese medicine, Acta Chinese Medicine and Pharmacology, 41 (2013) 84-87 (Chinese).

[13] H.D. Xie, K. Yang, H.D. Mu, S.D. Wei, Y.Y. Zhang, C.H. Liu, The effect of extracted scutellaria on renal interstitial fibrosis rats and its antioxidant mechanism, Chinese Journal of Integrated Traditional and Western Nephrology. 10 (2009) 240-242 (Chinese).

[14] R. Platt, M.H. Roscoe, F.W. Smith, Experimental renal failure, Clinical science (London, England: 1979). 11 (1952) 217-231.

[15] S.J. Sun, J.Y. Dai, J.W. Fang, X.J. Gou, H.J. Cao, N.N. Zheng, Y. Wang, W. Zhang, Y.Y. Zhang, W. Jia, Y.Y. Hu, Differences of Excess and Deficiency Zheng in Patients with Chronic Hepatitis B by Urinary Metabonomics, Evidence-Based Complementary and Alternative Medicine. Doi: 10.1155/2013/738245.

[16] X. Gao, E. Pujos-Guillot, J.F. Martin, P. Galan, C. Juste, W. Jia, J.L. Sebedio, Metabolite analysis of human fecal water by gas chromatography/mass spectrometry with ethyl chloroformate derivatization, Analytical biochemistry. 393 (2009) 163–175.

[17] MacKinnon M, Shurraw S, Akbari A, Knoll GA, Jaffey J, Clark HD: Combination therapy with an angiotensin receptor blocker and an ACE inhibitor in proteinuric renal disease: a systematic review of the efficacy and safety data. Am J Kidney Dis. 48(2006) 8-20.

[18] X.J. Wang, A.H. Zhang, G.L. Yan, W.J. Sun, Y. Han, H. Sun, Metabonomics and Proteomics Annotate Therapeutic Properties of Geniposide: Targeting and Regulating Multiple Perturbed Pathways, Plos One. 8(2013) 800-802.

[19] J.Y. Gao, Y.Y. Cheng, Application of Metabolomics Technology in Renal Diseases Research, Chinese Journal of Integrated Traditional and Western Nephrology. 12 (2011) 466-470 (Chinese).

[20] X.J. Wang. B. Yang, A.H. Zhang, H. Sun. G. Yan, Potential drug targets on insomnia and intervention effects of Jujuboside A through metabolic pathway analysis as revealed by UPLC/ESI-SYNAPT-HDMS coupled with pattern recognition approach, J Proteomics. 75(2012) 1411-1427.

15

[21] J.H. Shin, J.Y. Yang, B.Y. Jeon, Y.J. Yoon, S.N. Cho, Y.H. Kang, H. Ryu do, G.S. Hwang, (1)H NMR-based metabolomic profiling in mice infected with Mycobacterium tuberculosis, J Proteome Res. 10(2011) 2238–47.

[22] D.M. Wu, J. Lu, Y.L. Zheng, Y.L. Z. Zhou, Q. Shan, D.F. Ma, Purple sweet potato color repairs d-galactose-induced spatial learning and memory impairment by regulating the expression of synaptic proteins, Neurobiology of Learning & Memory. 90 (2008) 19-27.

[23] L. Ming, X. Hua, X. Ming, J. Ding, Q. Han, H. Gang, Impairments of astrocytes are involved in the d-galactose-induced brain aging, Biochemical & Biophysical Research Communications. 4 (2008) 1082–1087.

[24] M.M. Steed, S.C. Tyagi, Mechanisms of cardiovascular remodeling in hyperhomocysteinemia, Antioxid Redox Signal. 7 (2011) 1927-1943.

[25] M.J. Sarnak, A.S. Levey, A.C. Schoolwerth, J. Coresh, B. Culleton, L.L. Hamm, P.A. McCullough, B.L. Kasiske, E. Kelepouris, M.J. Klag, P. Parfrey, M. Pfeffer, L. Raij, D.J. Spinosa, P.W. Wilson, Kidney disease as a risk factor for development of cardiovascular disease: A statement from the American Heart Association Councils on Kidney in Cardiovascular Disease, High Blood Pressure Research, Clinical Cardiology, and Epidemiology and Prevention, Circulation. 108(2003) 2154–2169,

[26] A.S. Go, G.M. Chertow, D. Fan, C.E. McCulloch, C.Y. Hsu, Chronic kidney disease and the risks of death, cardiovascular events, and hospitalization, N Engl J Med. 351(2004) 1296–1305.

[27] J. Heinz, S. Kropf, C. Luley, J. Dierkes, Homocysteine as a risk factor for cardiovascular disease in patients treated by dialysis, A meta-analysis. Am J Kidney Dis. 54(2009) 478–489.

[28] L. Chen, R. H. Jia, C.J. Qiu, G. Ding, Hyperglycemia inhibits the uptake of dehydroascorbate in tubular epithelial cell, American Journal of Nephrology. 5(2005) 459-465.

[29] T. B. Zhou, G.P.C. Drummen, Y.H. Qin, The controversial role of retinoic acid in fibrotic diseases: analysis of involved signaling pathways, International Journal of Molecular Sciences. 1(2012)226-243.

[30] R.P. Aguilar, S. Genta, L. Oliveros, A. Anzulovich, M.S. Gimenez, S.S. Sanchez, Vitamin A deficiency injures liver parenchyma and alters the expression of hepatic extracellular matrix, Journal of Applied Toxicology. 29(2009) 214–222.

[31] T.B. Zhou, Y.H. Qin, Z.Y. Li, H.L. Xu, Y.J. Zhao, F.Y. Lei, All-trans retinoic Acid treatment is associated with prohibit in expression in renal interstitial fibrosis rats, Int. J. Mol. Sci. 13(2012) 2769–2782.

[32] G. Dixon, J. Nolan, N. Mcclenaghan, P.R. Flatt, P. Newsholme, A comparative study of amino acid consumption by rat islet cells and the clonal beta-cell line BRIN-BD11 - the functional significance of L-alanine, Journal of Endocrinology. 3 (2003)447-454.

[33] N.H. McClenaghan, C.R. Barnett, F.P.M. O'Harte, P.R. Flatt, Mechanisms of amino acid-induced insulin secretion from the glucose-responsive BRINBD11 pancreaticβ-cell line, J Endocrinol 15(1996)349–357.

[34] P. Manna, S.K. Jain, Phosphatidylinositol-3,4,5-Triphosphate and Cellular Signaling: Implications for Obesity and Diabetes, Cellular Physiology & Biochemistry. 35(2015)1253-1275.

[35] C. Pendaries, H. Tronchere, M. Plantavid, B. Payrastre, Phosphoinositide signaling disorders in human diseases, FEBS Lett. 546(2003) 25-3.

1   **Figures**
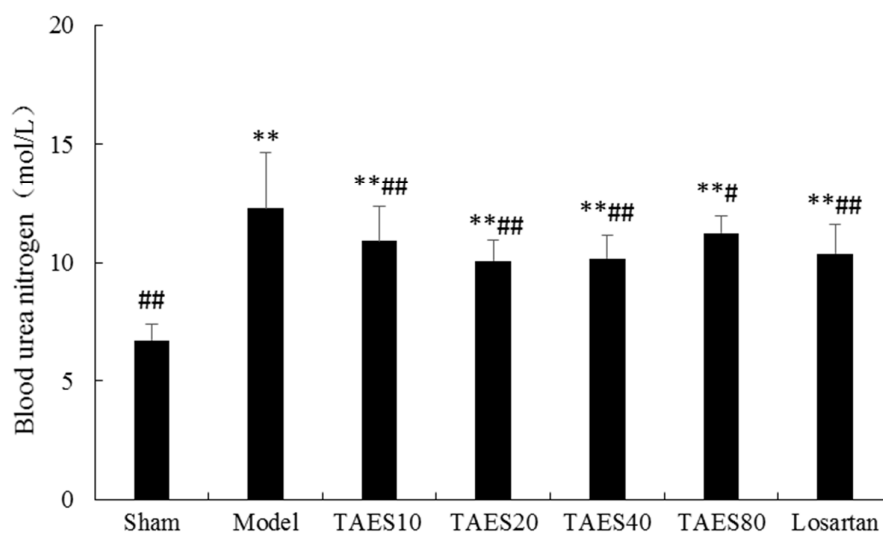
2

3   A
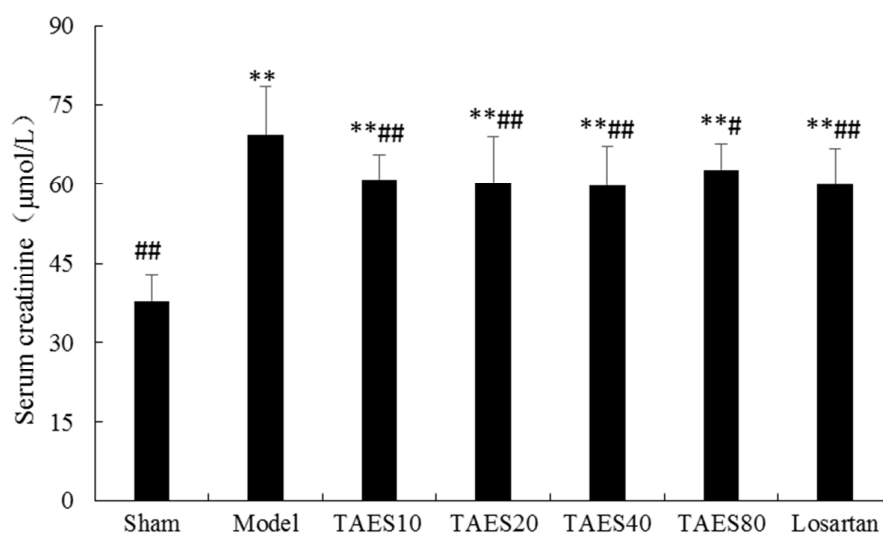
4

5   B

6   **Fig. 1.** TAES reduces the levels of BUN and Scr in 5/6 nephrectomy rats. After 5/6 nephrectomy rats were treated

7   with TAES at the doses of 10, 20, 40 and 80 mg/kg•d, respectively, for eight successive weeks, BUN (A) and Scr

8   (B) levels were analyzed. * P < 0.05, ** P < 0.01 compared with the sham group. # P < 0.05，## P < 0.01

9   compared with the control group. Data are expressed as mean ± SD. n = 15.

A Sham	B Model	C TAES10
D TAES20	E TAES40	F TAES80
G Losartan		
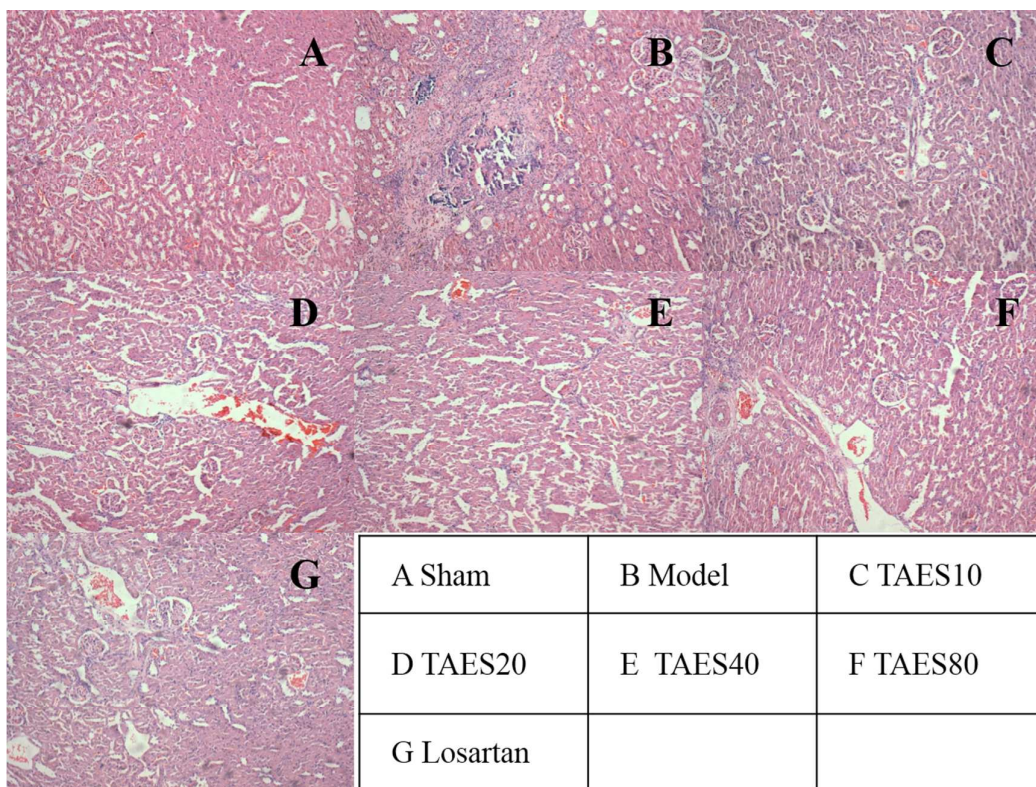
Fig. 2 Histological characteristics of renal tissue sections. 5/6 nephrectomy elicited features typical of CRF renal tissue in rats. However, these changes were evidently attenuated by TAES and losartan treatment for eight successive weeks. Figure C, D, E and F show renal tissues from groups administered with TAES at doses of 10, 20, 40 and 80 mg/kg·d, respectively. Figure G shows histological changes in renal tissue after losartan intervention. Original magnification × 100.
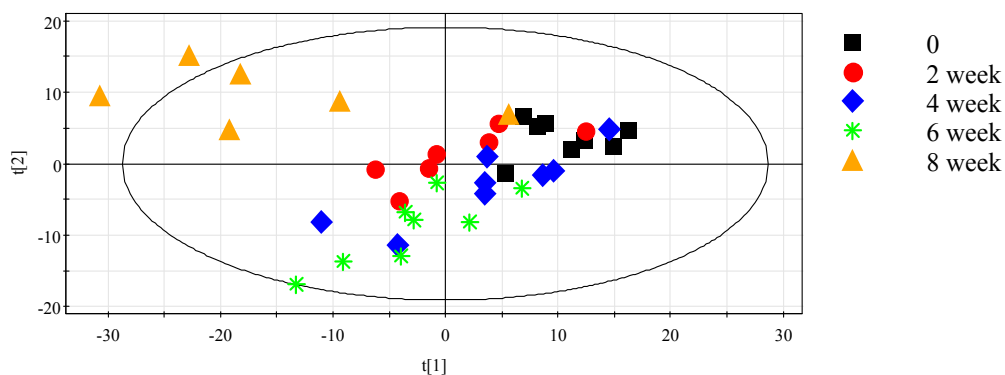
A
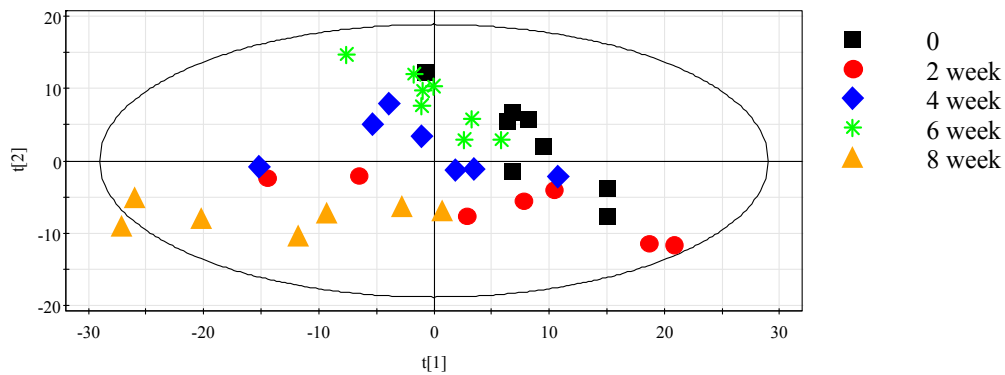
18

19   **B**

20   **Fig. 3** Score plot of PLS-DA derived from the GC/MS profiles of urine samples obtained from A: Control group,

21   B: Model group. In both the model and the sham group, distinct metabolic changes were apparent from Week 0

22   onwards.
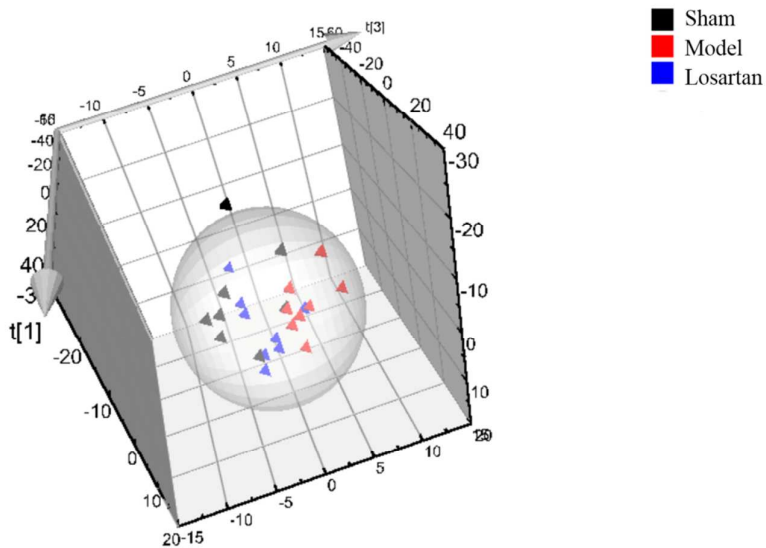
23

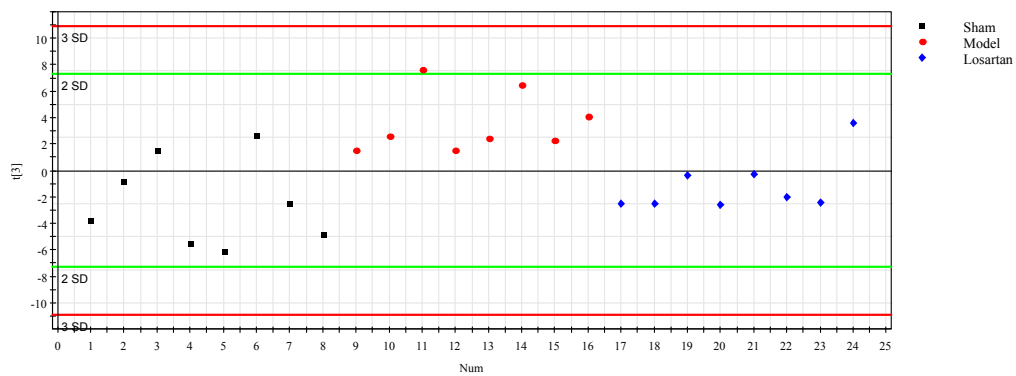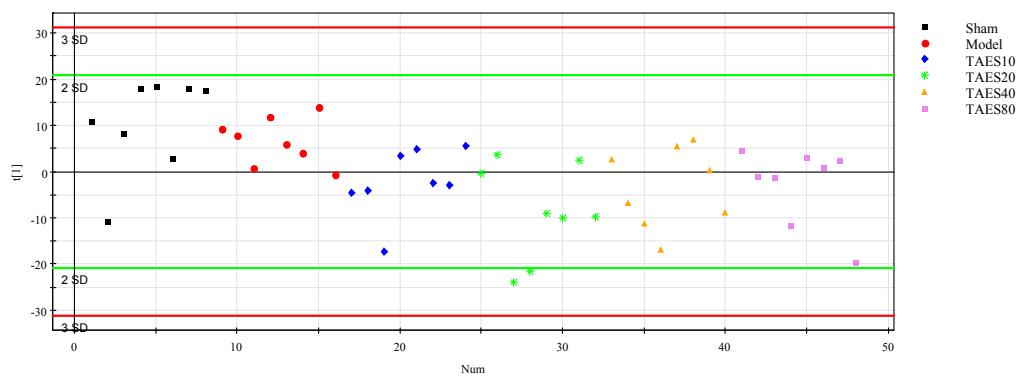24   A
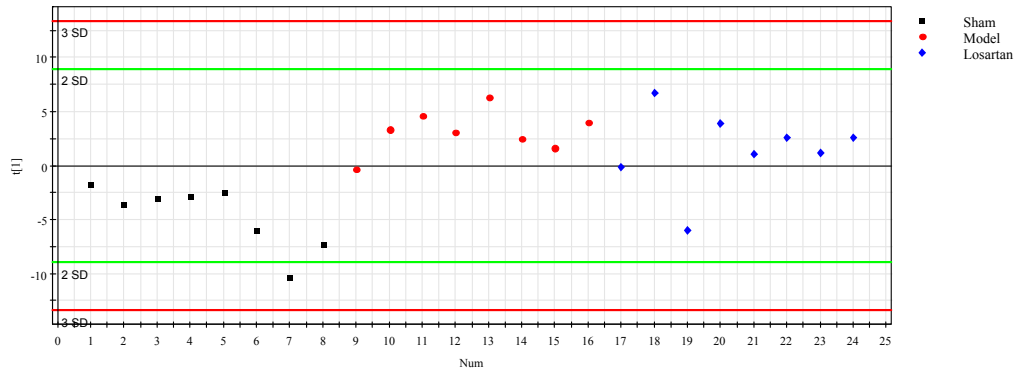
25

26 B (a)
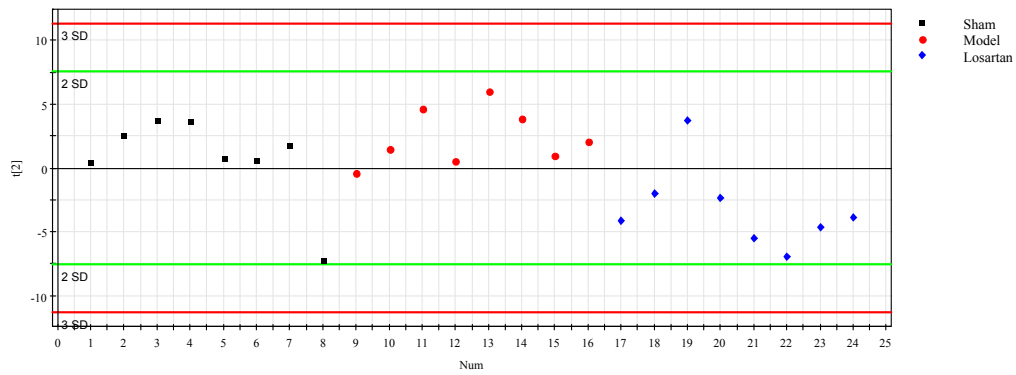
27

28 B (b)

29

30 B (c)

31 **Fig. 4** PLS-DA analyses of sham, model and losartan treatment group**.** A. Score plot of 3D-PLS-DA model. B.

32 Samples plotted in one dimension, (a) Score plot of PC 1, (b) Score plot of PC 2, (c) Score plot of PC 3.
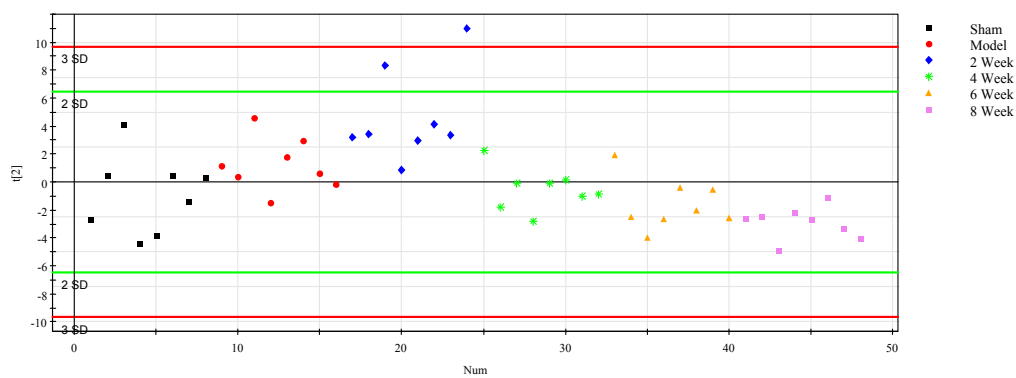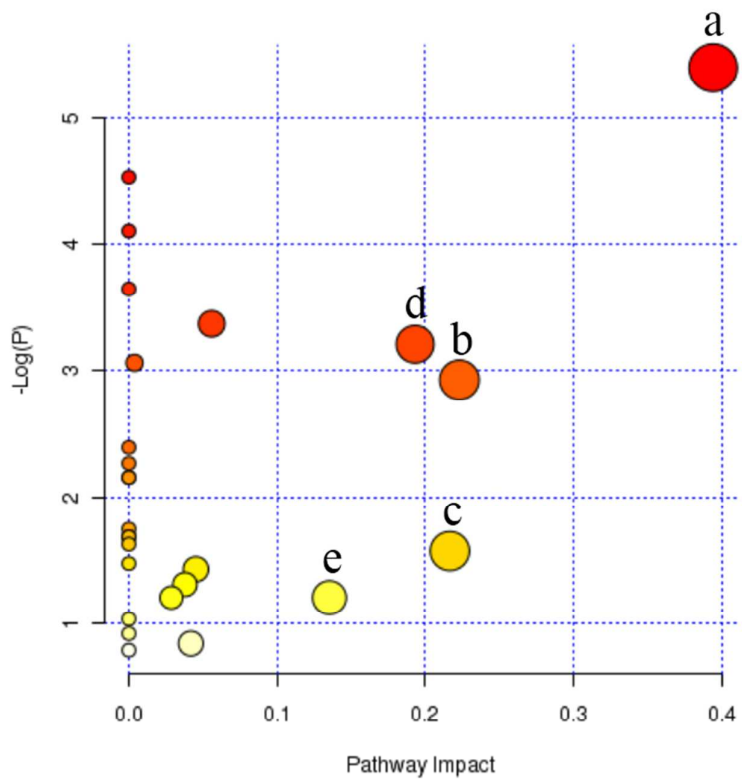
33

34 A
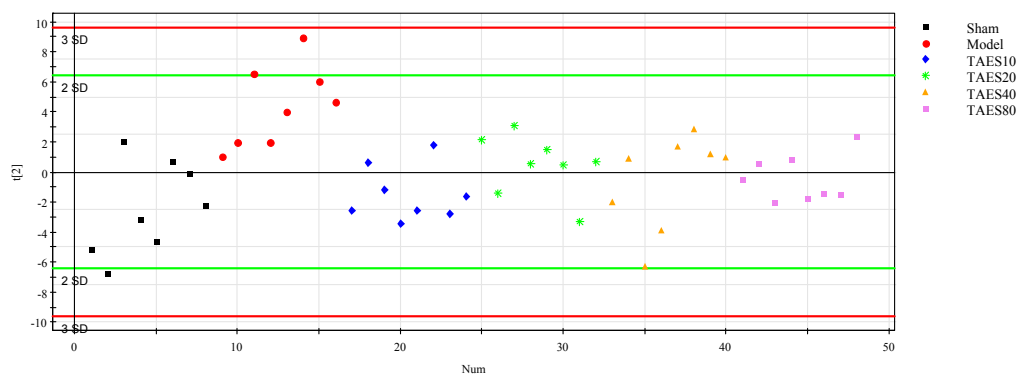
35

36 B

37 **Fig. 5** Score plots of PLS-DA model classifying the sham , mdel and TAES treatment group (10, 20, 40 and 80

38 mg/kg•d). A. Score plot of PC 1. B. Score plot of PC 2.
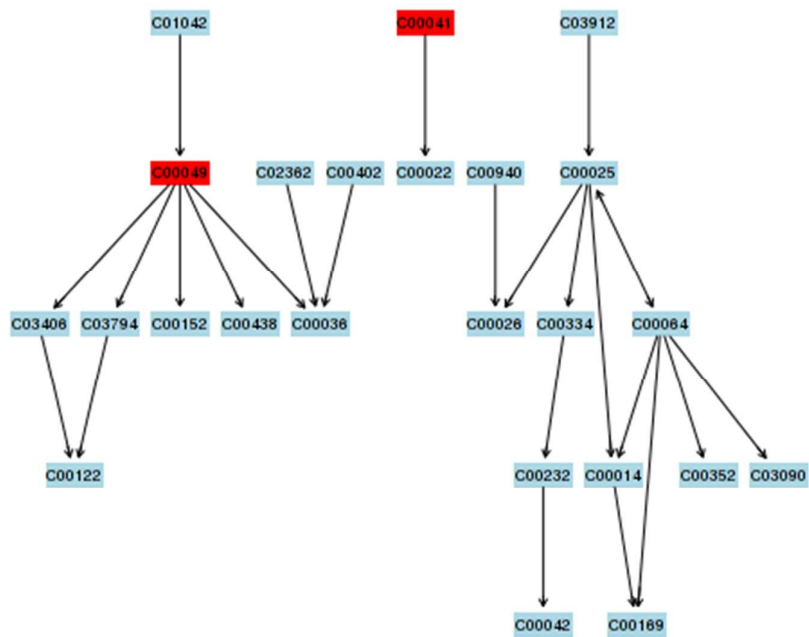

39

40 **Fig. 6** The trajectory of time-dependent changes in urinary metabolite profile (score plot of PC2) in the TAES 40

41 treatment group (the second, fourth, sixth, eighth week of treatment with TAES at a dosage of 40 mg/kg•d).
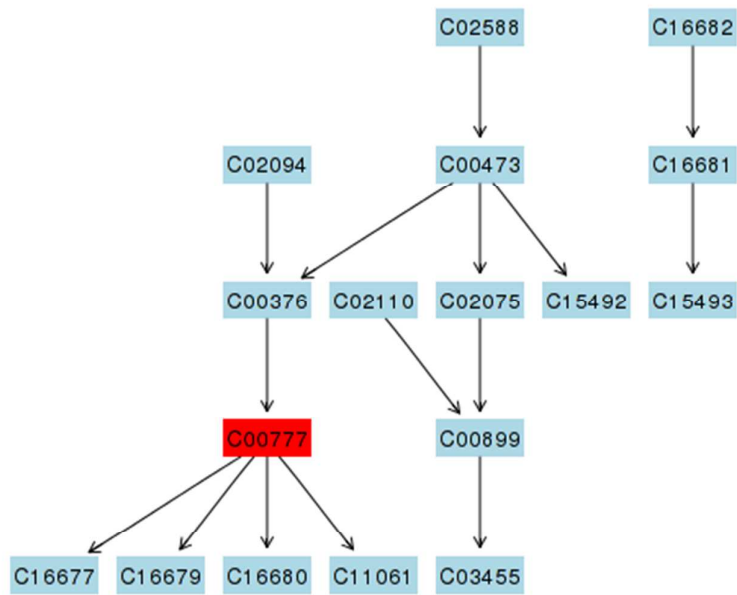
42

43   A

44

45   B (a)

C02588   C16682

C02094   C00473   C16681

C00376 C02110 C02075 C15492   C15493

C00777   C00899

C16677 C16679 C16680 C11061 C03455

46

47   B (b)

C04582   C00506   C00491

C15650   C05528   C01962

C15606

C01180   C08276

C00073

C00019

C01137   C00021

C00170   C00065   C00155

C04188   C02218   C02291

C00097   C00109

C00606   C00094   C00957

C05527   C00022   C00320   C05823
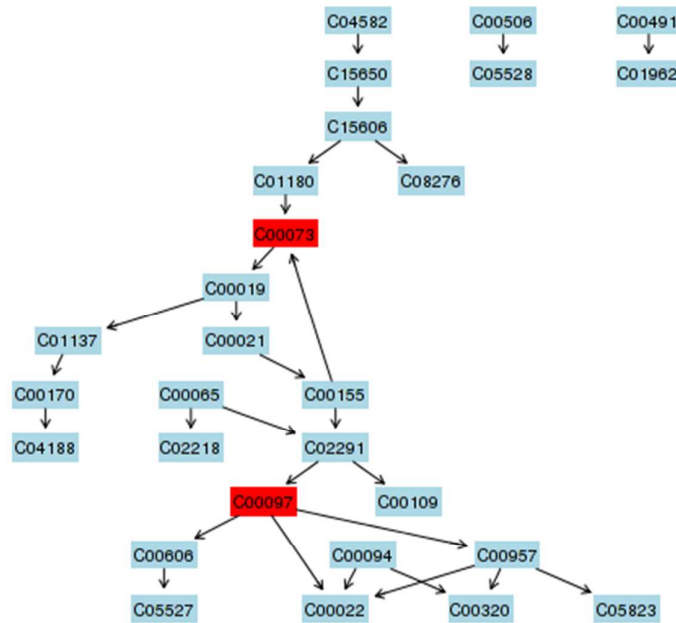
48

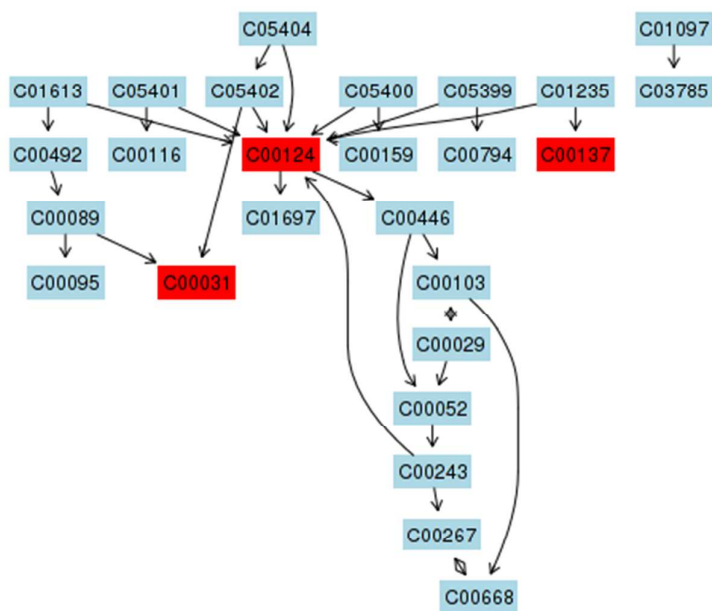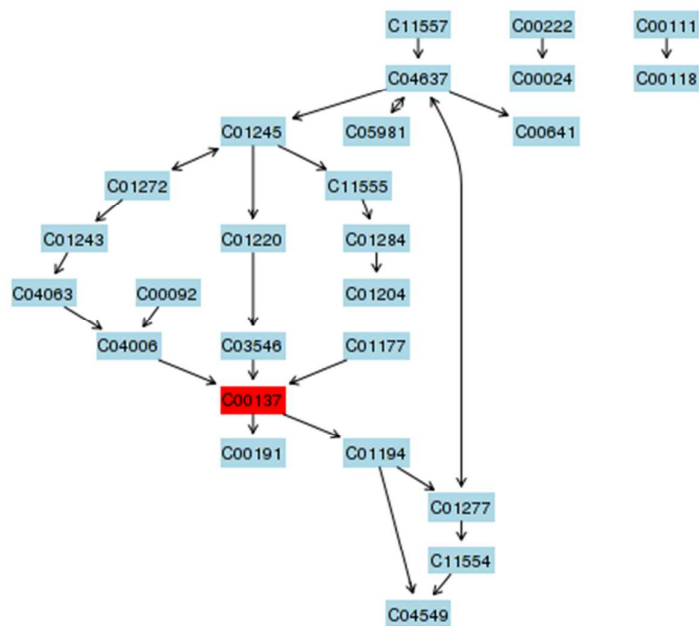49   B (c)

50

51   B (d)


52

53   B (e)

54   **Fig.7** Summary of pathway analysis. (A). a. galactose metabolism, b. cysteine and methionine metabolism, c.

55   retinol metabolism, d. alanine, aspartate and glutamate metabolism, e. inositol phosphate metabolism.

56   Identification of network pathway by MetPA software (B). Galactose metabolism (a), Cysteine and methionine

57   metabolism (b), Retinol metabolism (c), Alanine, aspartate and glutamate metabolism (d), Inositol phosphate

58   metabolism (e). Maps were generated using the reference map by KEGG (http://www.genome.jp/kegg/).
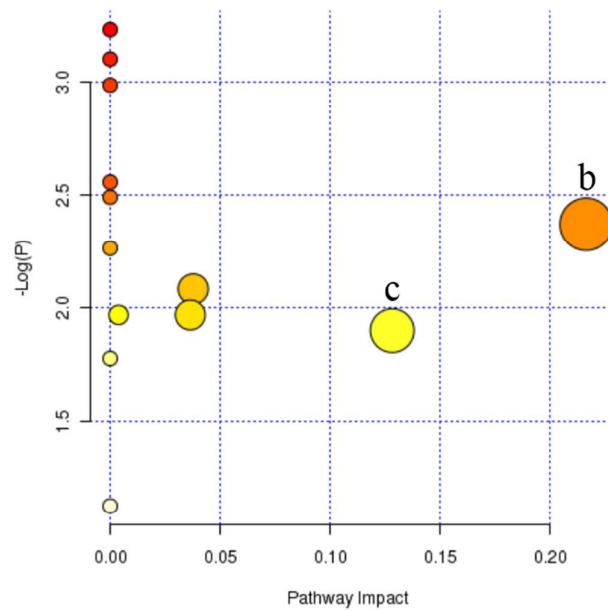
59

60   **Fig. 8.** Summary of pathway analysis. b. cysteine and methionine metabolism, c. retinol metabolism.